HHS Public Access

Author manuscript

Biomed Microdevices. Author manuscript; available in PMC 2018 September 25.

Published in final edited form as:

Biomed Microdevices. ; 19(4): 88. doi:10.1007/s10544-017-0225-9.

Interventional magnetic resonance imaging guided carotid embolectomy using a novel resonant marker catheter: demonstration of preclinical feasibility

Jeffrey K. Yang[1], **Andre M. Cote**[1], **Caroline D. Jordan**[1], **Sravani Kondapavulur**, **Aaron D. Losey**[1], **David McCoy**[1], **Andrew Chu**[2], **Jay F. Yu**[1], **Teri Moore**[1], **Carol Stillson**[1], **Fabio Settecase**[1], **Matthew D. Alexander**[1], **Andrew Nicholson**[1], **Daniel L. Cooke**[1], **Maythem Saeed**[1], **Dave Barry**[2], **Alastair J. Martin**[1], **Mark W. Wilson**[1], and **Steven W. Hetts**[1]

[1]Department of Radiology and Biomedical Imaging, UCSF, San Francisco, CA, USA

[2]Penumbra, Inc, Alameda, CA, USA

Abstract

To assess the visualization and efficacy of a wireless resonant circuit (wRC) catheter system for carotid artery occlusion and embolectomy under real-time MRI guidance *in vivo*, and to compare MR imaging modality with x-ray for analysis of qualitative physiological measures of blood flow at baseline and after embolectomy. The wRC catheter system was constructed using a MR compatible PEEK fiber braided catheter (Penumbra, Inc, Alameda, CA) with a single insulated longitudinal copper loop soldered to a printed circuit board embedded within the catheter wall. In concordance with IACUC protocol (AN103047), *in vivo* carotid artery navigation and embolectomy were performed in four farm pigs (40–45 kg) under real-time MRI at 1.5T. Industry standard clots were introduced in incremental amounts until adequate arterial occlusion was noted in a total of n=13 arteries. Baseline vasculature and restoration of blood flow were confirmed via MR and x-ray imaging, and graded by the Thrombolysis in Cerebral Infarction (TICI) scale. Wilcoxon signed-rank tests were used to analyze differences in recanalization status between DSA and MRA imaging. Successful recanalizations (TICI 2b/3) were compared to clinical rates reported in literature via binomial tests. The wRC catheter system was visible both on 5° sagittal bSSFP and coronal GRE sequence. Successful recanalization was demonstrated in 11 of 13 occluded arteries by DSA analysis and 8 of 13 by MRA. Recanalization rates based on DSA (0.85) and MRA (0.62) were not significantly different from the clinical rate of mechanical aspiration thrombectomy reported in literature. Lastly, a Wilcoxon signed rank test indicated no significant difference between TICI scores analyzed by DSA and MRA. With demonstrated compatibility and visualization under MRI, the wRC catheter system is effective for *in vivo* endovascular embolectomy, suggesting progress towards clinical endovascular interventional MRI.

Correspondence to: Steven W. Hetts.

Jeffrey K. Yang, Andre M. Cote and Caroline D. Jordan contributed equally to this work.

This work was presented in part at the 11th Interventional MRI Symposium, Baltimore, Maryland, October 7–8, 2016

Keywords

Interventional MRI; Stroke; Embolectomy; Wireless resonant marker

1 Introduction

Stroke is the leading cause of long-term disability and the fifth leading cause of death in the United States. In addition, stroke imposes a significant economic burden on the U.S. healthcare system: costs are projected to triple from $71.6 billion to $184.1 billion between 2012 and 2030. Each year approximately 795,000 people suffer from a new or recurrent stroke, of which 87% are acute ischemic strokes (Mozaffarian et al. 2016; Demaerschalk et al. 2010). Large vessel occlusion (LVO) ischemic strokes are particularly devastating due to the large amount of thrombus in the arteries at the base of the brain (e.g., internal carotid artery, middle cerebral artery) that supply blood to large brain territories (Smith et al. 2009). Administration of intravenous tissue plasminogen activator (tPA) is often insufficient in LVO to re-canalize the cerebral arteries, reperfuse the brain parenchyma, and prevent irreversible infarction. The large cerebral arteries can be accessed endovascularly with catheters through which blood clots can be mechanically removed. Recent randomized controlled trials have demonstrated the clinical superiority of x-ray angiography guided endovascular embolectomy to medical therapy alone in the first six hours of stroke onset, establishing mechanical thrombectomy as an equivalent or superior treatment method in an extended six hour stroke treatment window (Berkhemer et al. 2015; Campbell et al. 2015; Goyal et al. 2015; Saver et al. 2015; Jovin et al. 2015). Currently existing commercial catheters for mechanical thrombectomy can be divided into two main categories: stent retriever and aspiration catheters (Kang and Park 2017; Raychev and Saver 2012). The stent retrievers, including the Solitaire (*Medtronic, Minneapolis, MN*) and Trevo (*Stryker, Kalamazoo, MI*), utilize self-expanding nitinol or stainless steel stents that are deployed within the thrombus, entrapping the clot within the struts (Smith et al. 2008). The stent along with the thrombus are withdrawn together as a single unit. While stent retrievers have been shown to be clinically superior, they induce clot fragmentation that may cause distant emboli and utilize materials that are less likely to be MR safe. On the other hand, aspiration catheters, notably the Penumbra system, utilize a separator wire and vacuum aspiration to disrupt and remove occlusive clots (Penumbra Pivotal Stroke Trial Investigators 2009). These catheters are relatively inexpensive and have the ability to take out larger clots in a single piece, limiting clot fragmentation, but are prone to becoming clogged in the small intracranial arteries. These powerful clinical tools are now often paired with emergent MR imaging stroke protocols to further define recoverable areas of brain tissue, in addition to the DSA fluoroscopic guidance needed to direct the catheter system. MRI guidance for stroke treatment provides a number of substantial benefits, including measurements of soft-tissue perfusion and diffusion, which can guide the interventionalist to the areas that require intervention. Typical sequences for soft-tissue perfusion might include T2*-weighted GRE or EPI sequences that show susceptibility contrast over time, T1-weighted Dynamic Contrast Enhanced (DCE) sequences over time, or non-contrast-enhanced methods, such as Arterial Spin Labelling. Our long-term goal is to improve stroke treatment further by combining these two important loci of evaluation and treatment solely into the MR environment using

real-time MRI guidance as a substitute for the fluoroscopy suite. By allowing intra-procedural evaluation of brain parenchyma viability so that reperfusion therapy can be directed at living tissue and not at infarcted tissue, we believe that the total time for reperfusion of all affected brain areas would be reduced and would allow increased patient safety with fewer transfers and one fewer dedicated operative or imaging evaluation areas needed (Gonzalez 2006).

To facilitate clinical adoption of MRI guided interventions, endovascular devices must be reliably and accurately tracked and visualized (Hetts 2005; Düring and Novel 2014; Kramme et al. 2011). Currently, MR-guided catheter based interventions have clinical applications in the field of cardiac electrophysiology and are being tested for use in intravascular stent placement, chemo-ablation of tumors, and renal embolization (Henk et al. 2005; Wang 2015). These applications have demonstrated that MRI-based therapy can eliminate the need for prolonged ionized radiation exposure and offer a wealth of physiological and structural information. Compared to other imaging modalities, MRI provides biomarkers for physiological status of soft tissue and anatomical information on complex cardiovascular. Herein we pursue a tracking method consisting of MR compatible fiducial markers in isolated resonance circuits (Wendt and Wacker 2000; Zuehlsdorff et al. 2004). By tuning wire coil resonant circuits to the Larmor frequency of water protons in the external magnetic field, the circuit can couple with the transmit coil and increase the B1 field intensity by enhancing the exciting angle of protons in only a localized field surrounding the marker (Kuehne et al. 2003; Kaiser et al. 2015). Thus water protons adjacent to the circuit experience a much higher flip angle than the more distant surroundings. Using low flip angle sequences, semi-active resonant fiducial markers can be visualized under MR and have the potential to be used in current clinical applications that utilize active MR tracking (Dumoulin et al. 1993; Quick et al. 2005; Hillenbrand et al. 2004).

Applying resonant circuits to the tips of MR compatible catheters, we seek to develop a tool for endovascular navigation and thrombus removal, all performed under active tracking MR sequences with intermittent physiological evaluation of treatment progress. The aim of our current preclinical study is to assess the visualization and efficacy of a resonant circuit catheter system for MRI-guided carotid embolectomy *in vivo*. Previous studies have already demonstrated the viability of using similar applications for carotid stenting using MR guidance (Feng et al. 2005a, b). Our hope is to further this approach employing a similar animal model with the goal of aspiration embolectomy, rather than stent placement.

2 Methods

2.1 Wireless resonant marker catheter construction

A catheter with an outer diameter of 2.0 mm and an inner lumen diameter of 1.78 mm was designed to contain a wireless RF resonant marker on the outer surface of the distal catheter tip to enable active instrument visualization. Base catheter construction was performed using a 0.00075″ thick polytetrafluoroethylene (PTFE) liner with a single continuous 0.005″ diameter polyether ether ketone (PEEK) fiber thread wrapped circumferentially, then heat sealed with a layer of polyether block amide (Pebax) (0.003″) at 260 °C. The resonator was

constructed with an insulated 30 gauge longitudinal copper wire formed into a single loop measuring 55–65 mm in length and 2.5 mm in width (Quick et al. 2005). The single-loop coil was connected to a Pyralux flexible circuit board sheet (AP8515R, DuPont, Durham, NC) acting as a tunable capacitor with capacitance ranging from 55 to 100 pF (Fig. 1a). Trimming the flexible circuit board allowed for easy modification of length and area, thus modifying the capacitance of the system. The resonant frequency of the setup was then tuned to match the Larmor frequency (63.89 MHz) of the intended Philips Achieva 1.5 T MRI scanner. Once structurally complete, the resonant marker portion was thermally bonded using a Pebax coating to provide a stable environment surrounding the capacitor and flexible structural reinforcement (Fig. 1b).

In its completed form, the catheter with circuit and Pebax coating maintained torquability and flexibility similar to many commercial production catheters of similar diameter. Figure 2 visually demonstrates these properties in a completed prototype prior to use *in vivo*.

2.2 Artificial clot

Artificial clot material was initially developed to provide a realistic equivalent in consistency and resilience to actual blood clot for use in flow model simulations of circulatory systems for thrombectomy device testing (Kuehne et al. 2004; Chueh et al. 2011). We experimented with established clot analogues composed of bovine thrombin and autologous whole pig blood and with novel industrial clot equivalent used by device development companies (Shao et al. 2014). While autologous clot was readily available, post-delivery consistency was not reliable, thus we opted for the industry standard artificial clot (Duffy et al. 2016). The artificial clot material selected was composed using a mixture water, salt, plaster of Paris, dye coloring and a solidification chemical component (Concentric Medical, Mountain View, CA). Clots were sealed and refrigerated in airtight packaging until needed. Clot material was prepared just prior to insertion by forming multiple 15 mm × 3 mm × 3 mm individual clot pieces. Clots were then soaked in a 2% gadolinium aqueous solution for approximately 20 min prior to insertion to enhance MRI clot visualization and increase pliability for insertion similar to preparation used in previous studies (Robinson et al. 2013).

2.3 Animal subjects

Research was conducted under a protocol approved by the UCSF Committee on Animal Research (IACUC Protocol 103,047). Four 40–45 kg female Yorkshire farm pigs were acclimatized for 48 h prior to catheterization. Animals were placed under general anesthesia and oxygen saturation levels were continuously monitored. Prior to percutaneous femoral access, animals were intravenously heparinized at 0.2 mL/kg bodyweight (Heparin Sodium Injection, Fesenius Kabi, Lake Zurich, Il).

2.4 Imaging and catheterization protocol

All experiments were performed in a clinical hybrid interventional XMR suite combining an Achieva 1.5 T clinical MR scanner and an Integris V5000 C-arm DSA system (Philips Healthcare, Best, The Netherlands). The two image modalities were positioned in line and connected via a floating patient table that enabled rapid transfer between modalities. The workflow for the entire intervention is described in Fig. 3. A contrast enhanced MR

angiogram (CE-MRA), non-contrast in-flow MRA, and diffusion weighted imaging (DWI) sequence were acquired at baseline, after clot placement, and after embolectomy (Table 1).

Each animal was initially catheterized by an interventionalist (SWH, MWW, DLC) in the C-arm suite. A 3.67 mm arterial sheath (Cordis, Fremont, CA) was placed in the right femoral artery and used for advancement of intra-arterial catheters. Next, a 1.67 mm Berenstein II catheter (Cook, Bloomington, IN) was introduced through the right femoral artery sheath and positioned under fluoroscopic guidance in the common carotid artery (CCA) 2 cm proximal to the carotid artery bifurcation. Digital subtraction angiography (DSA) of the common carotid artery using a 10 mL injection of iodinated contrast (iohexol 350 mgI/mL, Omnipaque, GE healthcare, Waukesha, WI) was obtained prior to embolization. The catheter was then advanced beyond the bifurcation to select either the ascending pharyngeal artery (APA), supplying the rete mirabile and analogous to human internal carotid artery (ICA), or the external carotid artery (ECA). Using an over-the-wire exchange, the 5Fr diagnostic catheters were replaced with the 6 Fr straight tip resonant marker intervention catheters. Three to five individual clots were injected through the resonant marker catheters into either the ICA or ECA. Blood flow was evaluated by contrast injection following insertion of each clot. Once cessation of blood flow was satisfactory, the resonant marker catheter was pulled 2 cm proximal to the carotid bifurcation and a second DSA was performed to demonstrate unilateral carotid occlusion prior to embolectomy. Finally the resonant marker catheter was replaced into the selected occluded vessel branch with approximately 5 cm of distance from the tip of the resonant marker to the point of occlusion, awaiting later MR navigation and clot aspiration.

The animal subject was then transferred to the 1.5 T MR scanner for reassessment via GRE, DWI and 3D MRA. Following MR confirmation of carotid occlusion, the resonant marker catheter was advanced under real time MRI guidance using either a gradient echo (GRE) or a balanced steady-state free precession (bSSFP) sequence with a low flip angle. The catheter tip was visualized and advanced until abutting the clot. Firm manual aspiration was placed on the proximal hub of the catheter using a 60 mL syringe in order to engage the clot. While maintaining negative pressure, the catheter and clot were retracted from the common carotid artery to the aorta and then out through the femoral artery sheath.

Following aspiration embolectomy, 3D MRA and DWI were repeated to evaluate carotid blood flow and brain parenchyma. The animal was then shuttled back to the C-arm suite for a final post embolectomy DSA using 10 mL of Omnipaque-300 iodinated contrast. Animal subjects were euthanized immediately following the post-procedural DSA.

2.5 Quantitative and qualitative evaluation of vascular flow

MRA, DWI, and DSA were all recorded for baseline perfusion, post clot introduction, and post embolectomy. Levels of flow were measured at all three time points across several imaging modalities to confirm and analyze occlusion in the ICA, ECA, or CCA. We chose to analyze vessel recanalization via the validated Thrombolysis in Cerebral Infarction (TICI) scoring system. Revascularization was determined to be TICI 0, 1, 2a, 2b, or 3 (SWH) (Higashida et al. 2003). Following clinical standards, arteries with TICI outcomes of 2b or 3

were regarded as successful angiographic outcomes as evaluated by DSA. Arteries, status post embolectomy, with TICI outcomes of 2a or lower were deemed as unsuccessful.

Additional studies such as MR perfusion DCE and phase contrast MR, while potentially valid, were excluded from this initial study due to logistical limitations weighed against additional value of assessing vascular flow.

2.6 Physiological assessment using DWI

DWI images recorded at baseline, during occlusion, and after embolectomy were acquired with b-value = 800 s/mmˆ2. The apparent diffusion coefficient (ADC) values were determined at regions of interest (ROI) around at risk brain parenchyma supplied by the embolized blood vessels.

2.7 Statistical analysis

TICI scores were considered ordinal variables. Each imaging technique was compared to both spontaneous recanalization rate of 17% (Kassem-Moussa and Graffagnino 2002) and reported clinical success of mechanical thrombectomy of 71% (Jankowitz et al. 2012) using binomial probability tests. Arteries with a TICI score of 2b or 3 were considered successful (Writing Group Members et al. 2016) and 0, 1, or 2a were considered a failure (0). Comparisons between imaging technique and chance were collapsed over artery group. Wilcoxon signed-rank tests were used to analyze both differences between TICI scores post occlusion and post embolectomy, as well as differences in recanalization status between DSA and MRA. All tests were two-sided and a p-value of ≤ 0.05 was considered statistically significant. All statistical analysis was performed with STATA (Stata SE 13.1, StataCorp, College Station, Texas).

3 Results

Of the four animals in the study, the right carotid vasculatures of two animals were excluded. In the first animal, the right carotid artery was ruptured during catheter placement and the experiment was subsequently aborted. The right carotid artery of the second animal was not attempted due to experimental time constraints.

Successful embolus placement in either the ICA or ECA was achieved in six carotid vasculatures using 0.27 cm^3 of catheter-delivered artificial blood clot. In the four swine, 6/6 ICA, 6/6 ECA, and 1/1 CCA arteries were occluded. The occlusion was then re-demonstrated on MRA in 6/6 ICA, 5/6 ECA, and 1/1 CCA cases. Of note, MR imaging was often limited at this stage due to the loss of vascular flow in the carotid arteries. As flow slowed, the ability of inflow MRA to represent stagnant blood flow was reduced. In this case, the relative absence of vessels on MRA was interpreted as halted flow with confirmation by post-occlusion DSA that demonstrated abrupt cessation of contrast flow and arterial reflux in the remaining patent carotid branch.

During the embolectomy procedure, the resonator catheter was successfully visualized under real-time bSSFP or 5° GRE. For both sequences, it was determined that an oblique sagittal and coronal plane would best visualize the resonator catheter and the course of the common

carotid artery, respectively. Suction embolectomy was then performed under real time bSSFP MR guidance. The resonance signal from the single-loop coil allowed navigation from the common carotid artery, proximal to the carotid bifurcation, to the clot and aspirate clot material. Resonant marker catheters were continuously visualized during aspiration with an oblique sagittal plane bSSFP sequence. A demonstration of visualization across each orientation of navigational scan as well as images from active image tracking are shown in Fig. 4. Additionally, Fig. 5 demonstrates catheter visualization pre-embolectomy and during aspiration with clot noted as a filling defect in the lumen.

Degrees of occlusion and of recanalization were verified with both x-ray DSA and MRA. Vasculature at baseline, post occlusion, and post embolectomy from a single experiment are shown in Fig. 6 and Fig. 7 under both imaging modalities.

Restoration of flow was graded in each individual artery. The DSA and MRA images were both analyzed for each artery of interest and an individual TICI score was assigned. Relevant TICI scores analyzed from DSA and MRA are outlined in Fig. 8 and Fig. 9, respectively. TICI score trends demonstrated a high rate of success in our ability to recanalize the occluded vessels (TICI restored to 2b or 3).

We demonstrated successful recanalization in 11 of 13 occluded arteries by DSA analysis and 8 of 13 arteries by MRA analysis. Per experiment protocol, no second attempt was made to remove the emboli. In these 13 arteries considered, clot was successfully removed from 6/6 ECA branches, 4/6 ICA branches, and 1/1 CCA branches. Successful embolecto-my as re-demonstrated on MRA in 4/6 ICA, 4/6 ECA, and 0/1 CCA. When compared with spontaneous recanalization in stroke patients, binomial tests indicated that the proportion of successful recanalization based on DSA of 0.85 (11 of 13) and MRA of 0.62 (8 of 13) were both significantly higher than the expected 0.17 ($p < 0.001$). Additionally, binomial testing comparing DSA (0.85) and MRA (0.62) to the clinical rates of success in ELVO embolectomy (Chueh et al. 2011) showed no significant difference with $p = 1.00$ and $p = 0.16$, respectively. A Wilcoxon signed-rank test confirmed significant TICI score differences between occluded and post embolectomy arteries (DSA: $p = 0.00148$, MRA: $p = 0.0222$). Lastly, a Wilcoxon signed-rank test resulted in no significant difference between DSA and MRA ($z = 1.494$, $p = 0.135$). When investigating differences for each artery type, no significant differences were found between DSA and MRA (ECA: $p = 0.157$, ICA: $p = 0.876$, CCA: $p = 0.317$).

In DWI and ADC analysis, one of the swine subjects did develop transient regional changes in ADC values with baseline, post-occlusion, and post-embolectomy values at 828.90, 588.29, and 794.97, respectively. In other subjects, image quality was limited and no definite diffusion changes could be confirmed.

4 Discussion

This study demonstrates the feasibility of using an MR conditional endovascular catheter with wireless resonant marker visualization in retrieving an intra-arterial thrombus in a simulated ELVO stroke. The resonant circuit catheter system was visualized via signal

amplification at low flip angles *in vivo*, and allowed for real-time MR guided catheter tracking during embolectomy. Our success rates in embolectomy in both the ICA and ECA subgroups were excellent, achieving revascularization rates similar to clinical procedures in human patients. The resonator catheter's PEEK braided PTFE shaft provided a durable and MR compatible substrate that retained strength throughout multiple experimental repetitions. Our study demonstrates a novel porcine model for human intracranial arterial procedures simulating ELVO stroke in an MR environment when used in conjunction with our MR compatible resonant marker system.

While this study did demonstrate feasibility of visualization, the stroke model was challenging for several reasons. Animal models of ELVO strokes are often limited by locating both the necessary cerebral vessel diameter (2–5 mm) in a subject with sufficient cortical matter to demonstrate significant infarction (Gralla et al. 2006). Pigs have cervical blood vessels similar in size to human brain blood vessels, and thus can provide an acceptable analogue for device testing. Further refinement is needed in our porcine model. While we were able to demonstrate the feasibility of the porcine neurovascular model for performance of the embolectomy, we were not able to demonstrate significant changes on DWI imaging during embolization. Due to the biological model and robust collateral perfusion seen in the porcine brain through the rete mirabile and posterior circulation, we did not expect transient carotid occlusion to cause regional brain infarcts. Previous studies have demonstrated that complete occlusion of the ECA yielded no significant changes in cerebral blood flow in an identical porcine model, owed at least in part to ECA and ICA anastomoses (Mangla et al. 2015). Thusly, we were not expecting significant changes in this imaging. In our DWI and ADC analysis, one of the swine subjects did develop transient regional changes in ADC values, but not sufficient to evolve a cortical or subcortical infarction. In short, human-like changes in perfusion are not evident in the porcine brain even with 100% occlusion of a single ICA, but may still be sufficient for quantitative evaluation of ADC data, a key imaging biomarker for physiological viability in human systems (Martin et al. 2005; Schellinger et al. 2010). Further, even if the porcine model perfectly emulated a human cerebrovascular blood supply, the time frame from complete unilateral occlusion to DWI sequence acquisition was approximately 30 to 45 min, which is often less than the time needed to see acute imaging changes in humans.

Our imaging sequence selection was also limited in this preliminary study. As this was a feasibility study in which we were comparing the abilities of MR against the x-ray gold standard visualization with minimal navigation, we did not perform phase contrast MR imaging to fully characterize the tissue surrounding the blockage. Rather, we elected for angiographic methods of assessing revascularization that were analogous to those commonly used with DSA. Additionally, an MR perfusion protocol was deemed beyond the scope of this experimental design and thus was excluded. While MR perfusion could have provided interesting supplemental information, we prioritized contrast enhanced MRA over DCE perfusion as a rapid way to evaluate the arterial anatomy. Given that the contrast enhanced MRA would be repeated several times during the procedure we did not want to administer additional MR contrast for DCE perfusion. Rather, we relied on DWI measures for evaluating the status of the brain. In future studies, additional scans, and therefore additional

time for cell death to occur, could provide additional insight into the biological accuracy of the swine as a model of the human neurovascular system.

It should be noted that DSA assessment in this study also proved to be an equal or marginally superior method of vascular occlusion assessment as compared to MRI in our swine model. We believe this effect to be less of a comment on the ability of each assessment method and more a factor of timing in the experiment. With any artificial or natural occlusion of vasculature, endogenous plasminogens already found in the blood stream of the swine model attempt to disrupt the blockage. Given that DSA was performed after MRI assessment during post embolectomy analysis, we theorize that biological plasminogen had additional access to vasculature and ability to break up clots during the move. This could have biased the results toward DSA. This effect, as seen in human stroke patients, is further enhanced as blood flow is restored to previously inaccessible smaller areas of clot during the endogenous clot dissolution process.

The device design itself can also be limiting in this study as we opted for a simplified and lower profile device that did not use a decoupling circuit. The lack of a decoupling circuit during RF transmission, and the local flip angle amplification could result in high flip angles and increased local specific absorption rate (SAR). One possible solution is to add anti-parallel decoupling diodes, which are currently available as thin wafers, to the circuit. While the device is functional in its current iteration, the addition of crossed diodes may be necessary for enhanced safety and clinical implementation. Another limitation was the time it took to manually determine the location of the resonant marker. In a previous study, an MR-tracking sequence that automatically updated the imaging location and plane was implemented in combination with a wireless resonant circuit (Rube et al. 2014), based on a prior tracking sequence used with active markers (Dumoulin et al. 1993). This could be implemented in future studies.

In addition to limitations in physiological imaging, our study was limited by small sample size. Although sufficient trials were conducted to indicate the feasibility of MR-guided carotid embolectomy, overall efficacy of MR-guided embolectomy as compared to x-ray guided embolectomy was beyond the scope of this study. From the small number of cases performed, we can see that achieving TICI 2b to 3 recanalization is possible with MR-guided embolectomy, but cannot comment on the robustness of this nascent technique as compared to the well-developed clinical standard of x-ray guided embolectomy.

This study was designed to address building a framework for further experiments to evaluate and refine catheter design based on visualization, but was not intended to directly evaluate long distance navigation under real time MR imaging. A next step in the catheter development process is to use our existing devices for the full navigation from femoral access to the carotid artery occlusion site, instead of the last few centimeters prior to clot. The advent of MRI-conditional guidewires from such companies as MaRVis (Hanover, Germany) and Nano4Imaging (Aachen, Germany) will permit full navigation from access site to arterial occlusion site under MRI guidance. To add greater clinical context to these navigation experiments we expect to address time to reperfusion, an important benchmark of achievement for stroke related interventions. With repeated trials, we hope to build a data set

with sufficient x-ray fluoroscopic and MRI-guided procedures to demonstrate similarity in reperfusion times.

In conclusion, our study demonstrates the feasibility of a wireless resonator circuit catheter system *in vivo* for the performance of neurovascular embolectomy using real-time MRI guidance. This sets the stage for more robust device and imaging technique development.

4.1 Advances in knowledge

1. Using the wireless resonant catheter system for carotid artery embolectomy under real-time MR guidance is feasible and comparable to standard x-ray guided intervention.

2. Due to enlargement of transmitted flip angle in the neighborhood of the wRC catheter tip, the tip appears hyperin-tense and is easy to locate under MRI guidance *in vivo*.

3. MRA evaluation of flow at baseline, during occlusion, and post embolectomy was comparable to the x-ray gold standard.

4.2 Implications for patient care

MR-guided interventions provide real-time imaging biomarkers and a wealth of physiological information not available with x-ray guidance alone. This additional data provides quantitative measures of success and allows the interventionalist to determine whether further intervention is necessary. It is possible to construct MRI-based catheters for navigating to and treating ischemic stroke by removing clots from blocked vessels in the neck.

4.3 Summary statement

Our study demonstrates the feasibility of using a wireless resonant circuit (wRC) catheter for *in vivo* MR guided carotid embolectomy and is a step toward clinical endovascular interventional MRI, wherein the interventionalist has intra-procedural access to imaging biomarkers.

Acknowledgments

This work was supported by the National Institute of Biomedical Imaging and Bioengineering grants R01EB012031 and R21EB020283 and the National Center for Advancing Translational Sciences grant UL1TR000004. The authors thank Penumbra, Inc., for in-kind provision of catheter shafts, materials, and engineering expertise.

References

Berkhemer OA, Fransen PS, Beumer D, van den Berg LA, Lingsma HF, Yoo AJ, Schonewille WJ, Vos JA, Nederkoorn PJ, Wermer MJ, van Walderveen MA, Staals J, Hofmeijer J, van Oostayen JA, Lycklama a Nijeholt GJ, Boiten J, Brouwer PA, Emmer BJ, de Bruijn SF, van Dijk LC, Kappelle LJ, Lo RH, van Dijk EJ, de Vries J, de Kort PL, van Rooij WJ, van den Berg JS, van Hasselt BA, Aerden LA, Dallinga RJ, Visser MC, Bot JC, Vroomen PC, Eshghi O, Schreuder TH, Heijboer RJ, Keizer K, Tielbeek AV, den Hertog HM, Gerrits DG, van den Berg-Vos RM, Karas GB, Steyerberg EW, Flach HZ, Marquering HA, Sprengers ME, Jenniskens SF, Beenen LF, van den Berg R, Koudstaal PJ, van Zwam WH, Roos YB, van der Lugt A, van Oostenbrugge RJ, Majoie CB, Dippel

DW, MR CLEAN Investigators. A randomized trial of intraarterial treatment for acute ischemic stroke. N Engl J Med. 2015; 372(1):11–20. [PubMed: 25517348]

Campbell BC, Mitchell PJ, Kleinig TJ, Dewey HM, Churilov L, Yassi N, Yan B, Dowling RJ, Parsons MW, Oxley TJ, Wu TY, Brooks M, Simpson MA, Miteff F, Levi CR, Krause M, Harrington TJ, Faulder KC, Steinfort BS, Priglinger M, Ang T, Scroop R, Barber PA, McGuinness B, Wijeratne T, Phan TG, Chong W, Chandra RV, Bladin CF, Badve M, Rice H, de Villiers L, Ma H, Desmond PM, Donnan GA, Davis SM, EXTEND-IA Investigators. Endovascular therapy for ischemic stroke with perfusion-imaging selection. N Engl J Med. 2015; 372(11):1009–1018. [PubMed: 25671797]

Chueh JY, Wakhloo AK, Hendricks GH, Silva CF, Weaver JP, Gounis MJ. Mechanical characterization of thromboemboli in acute is-chemic stroke and laboratory embolus analogs. AJNR Am J Neuroradiol. 2011; 32(7):1237–1244. [PubMed: 21596804]

Demaerschalk BM, Hwang HM, Leung G. US cost burden of ische-mic stroke: A systematic literature review. Am J Manag Care. 2010; 16(7):525–533. [PubMed: 20645668]

Duffy S, Farrell M, McArdle K, Thornton J, Vale D, Rainsford E, Morris L, Liebeskind DS, MacCarthy E, Gilvarry M. Novel methodology to replicate clot analogs with diverse composition in acute ischemic stroke. J Neurointerv Surg. 2017; 9(5):486–491. https://doi.org/10.1136/neurintsurg-2016-012308. [PubMed: 27127231]

Dumoulin CL, Souza SP, Darrow RD. Real-time position monitoring of invasive devices using magnetic resonance. Magn Reson Med. 1993; 29(3):411–415. [PubMed: 8450752]

Düring, K., Novel, MR. Safe Guidewires for MRI-Guided Interventions; Interventional MRI Symposium; Leipzig. 2014; p. 30

Feng L, Dumoulin CL, Dashnaw S, Darrow RD, Guhde R, DeLaPaz RL, Bishop PL, Pile-Spellman J. Transfemoral catheterization of carotid arteries with real-time MR imaging guidance in pigs. Radiology. 2005a; 234(2):551–557. [PubMed: 15591433]

Feng L, Dumoulin CL, Dashnaw S, Darrow RD, DeLaPaz RL, Bishop PL, Pile-Spellman J. Feasibility of stent placement in carotid arteries with real-time MR imaging guidance in pigs. Radiology. 2005b; 234(2):558–562. [PubMed: 15591432]

Gonzalez RG. Imaging-guided acute ischemic stroke therapy: From “time is brain” to “physiology is brain”. AJNR Am J Neuroradiol. 2006; 27(4):728–735. [PubMed: 16611754]

Goyal M, Demchuk AM, Menon BK, Eesa M, Rempel JL, Thornton J, Roy D, Jovin TG, Willinsky RA, Sapkota BL, Dowlatshahi D, Frei DF, Kamal NR, Montanera WJ, Poppe AY, Ryckborst KJ, Silver FL, Shuaib A, Tampieri D, Williams D, Bang OY, Baxter BW, Burns PA, Choe H, Heo JH, Holmstedt CA, Jankowitz B, Kelly M, Linares G, Mandzia JL, Shankar J, Sohn SI, Swartz RH, Barber PA, Coutts SB, Smith EE, Morrish WF, Weill A, Subramaniam S, Mitha AP, Wong JH, Lowerison MW, Sajobi TT, Hill MD, ESCAPE Trial Investigators. Randomized assessment of rapid endovascular treatment of ischemic stroke. N Engl J Med. 2015; 372(11):1019–1030. [PubMed: 25671798]

Gralla J, Schroth G, Remonda L, Fleischmann A, Fandino J, Slotboom J, Brekenfeld C. A dedicated animal model for mechanical thrombectomy in acute stroke. AJNR Am J Neuroradiol. 2006; 27(6):1357–1361. [PubMed: 16775297]

Henk CB, Higgins CB, Saeed M. Endovascular interventional MRI. J Magn Reson Imaging. 2005; 22(4):451–460. [PubMed: 16161076]

Hetts SW. Interventional magnetic resonance imaging: The revolution begins. Appl Radiol. 2005; 34:84–91.

Higashida RT, Furlan AJ, Roberts H, Tomsick T, Connors B, Barr J, Dillon W, Warach S, Broderick J, Tilley B, Sacks D, Technology assessment Committee of the American Society of interventional and therapeutic neuroradiology, technology assessment Committee of the Society of interventional radiology. Trial design and reporting standards for intra-arterial cerebral thrombolysis for acute ischemic stroke. Stroke. 2003; 34(8):e109–e137. [PubMed: 12869717]

Hillenbrand CM, Elgort DR, Wong EY, Reykowski A, Wacker FK, Lewin JS, Duerk JL. Active device tracking and high-resolution intravascular MRI using a novel catheter-based, opposed-solenoid phased array coil. Magn Reson Med. 2004; 51(4):668–675. [PubMed: 15065238]

Jankowitz B, Aghaebrahim A, Zirra A, Spataru O, Zaidi S, Jumaa M, Ruiz-Ares G, Horowitz M, Jovin TG. Manual aspiration thrombectomy: Adjunctive endovascular recanalization technique in acute stroke interventions. Stroke. 2012; 43(5):1408–1411. [PubMed: 22382156]

Jovin TG, Chamorro A, Cobo E, de Miquel MA, Molina CA, Rovira A, San Roman L, Serena J, Abilleira S, Ribo M, Millan M, Urra X, Cardona P, Lopez-Cancio E, Tomasello A, Castano C, Blasco J, Aja L, Dorado L, Quesada H, Rubiera M, Hernandez-Perez M, Goyal M, Demchuk AM, von Kummer R, Gallofre M, Davalos A, REVASCAT trial investigators. Thrombectomy within 8 hours after symptom onset in ischemic stroke. N Engl J Med. 2015; 372(24):2296–2306. [PubMed: 25882510]

Kaiser M, Detert M, Rube MA, El-Tahir A, Elle OJ, Melzer A, Schmidt B, Rose GH. Resonant marker design and fabrication techniques for device visualization during interventional magnetic resonance imaging. Biomed Tech (Berl). 2015; 60(2):89–103. [PubMed: 25460277]

Kang DH, Park J. Endovascular stroke therapy focused on stent retriever thrombectomy and direct clot aspiration: Historical review and modern application. J Korean Neurosurg Soc. 2017; 60(3):335–347. [PubMed: 28490161]

Kassem-Moussa H, Graffagnino C. Nonocclusion and spontaneous recanalization rates in acute ischemic stroke: A review of cerebral angiography studies. Arch Neurol. 2002; 59(12):1870–1873. [PubMed: 12470173]

Kramme, R.Hoffmann, K., Pozos, RS., editors. Springer Handbook of Medical Technology. Springer Berlin Heidelberg; Berlin, Heidelberg: 2011. p. 477-501.

Kuehne T, Fahrig R, Butts K. Pair of resonant fiducial markers for localization of endovascular catheters at all catheter orientations. J Magn Reson Imaging. 2003; 17(5):620–624. [PubMed: 12720274]

Kuehne T, Weiss S, Brinkert F, Weil J, Yilmaz S, Schmitt B, Ewert P, Lange P, Gutberlet M. Catheter visualization with resonant markers at MR imaging-guided deployment of endovascular stents in swine. Radiology. 2004; 233(3):774–780. [PubMed: 15498900]

Mangla S, Choi JH, Barone FC, Novotney C, Libien J, Lin E, Pile-Spellman J. Endovascular external carotid artery occlusion for brain selective targeting: A cerebrovascular swine model. BMC Res Notes. 2015; 8:808. [PubMed: 26689288]

Martin AJ, Saloner DA, Roberts TP, Roberts H, Weber OM, Dillon W, Cullen S, Halbach V, Dowd CF, Higashida RT. Carotid stent delivery in an XMR suite: Immediate assessment of the physiologic impact of extracranial revascularization. AJNR Am J Neuroradiol. 2005; 26(3):531–537. [PubMed: 15760861]

Penumbra Pivotal Stroke Trial Investigators. The penumbra pivotal stroke trial: Safety and effectiveness of a new generation of mechanical devices for clot removal in intracranial large vessel occlusive disease. Stroke. 2009; 40(8):2761–2768. [PubMed: 19590057]

Quick HH, Zenge MO, Kuehl H, Kaiser G, Aker S, Massing S, Bosk S, Ladd ME. Interventional magnetic resonance angiography with no strings attached: Wireless active catheter visualization. Magn Reson Med. 2005; 53(2):446–455. [PubMed: 15678524]

Raychev R, Saver JL. Mechanical thrombectomy devices for treatment of stroke. Neurol Clin Pract. 2012; 2(3):231–235. [PubMed: 23634369]

Robinson RA, Herbertson LH, Sarkar Das S, Malinauskas RA, Pritchard WF, Grossman LW. Limitations of using synthetic blood clots for measuring in vitro clot capture efficiency of inferior vena cava filters. Med Devices (Auckl). 2013; 6:49–57. [PubMed: 23690701]

Rube MA, Holbrook AB, Cox BF, Houston JG, Melzer A. Wireless MR tracking of interventional devices using phase-field dithering and projection reconstruction. Magn Reson Imaging. 2014; 32(6):693–701. https://doi.org/10.1016/j.mri.2014.03.007 Epub 2014 Mar 17. [PubMed: 24721007]

Saver JL, Goyal M, Bonafe A, Diener HC, Levy EI, Pereira VM, Albers GW, Cognard C, Cohen DJ, Hacke W, Jansen O, Jovin TG, Mattle HP, Nogueira RG, Siddiqui AH, Yavagal DR, Baxter BW, Devlin TG, Lopes DK, Reddy VK, du Mesnil de Rochemont R, Singer OC, Jahan R, SWIFT PRIME investigators. Stent-retriever thrombectomy after intravenous t-PA vs. t-PA alone in stroke. N Engl J Med. 2015; 372(24):2285–2295. [PubMed: 25882376]

Schellinger PD, Bryan RN, Caplan LR, Detre JA, Edelman RR, Jaigobin C, Kidwell CS, Mohr JP, Sloan M, Sorensen AG, Warach S. Therapeutics and technology assessment Subcommittee of the American Academy of neurology. Evidence-based guideline: The role of diffusion and perfusion MRI for the diagnosis of acute ischemic stroke: Report of the therapeutics and technology assessment subcommittee of the american academy of neurology. Neurology. 2010; 75(2):177–185. [PubMed: 20625171]

Shao Q, Zhu L, Li T, Li L, Li D, Zhang J, Ren W, Wu L. New method of thrombus preparation using a fluid model for evaluation of thrombectomy devices in a swine model. Thromb Res. 2014; 134(5): 1087–1092. [PubMed: 25201003]

Smith WS, Sung G, Saver J, Budzik R, Duckwiler G, Liebeskind DS, Lutsep HL, Rymer MM, Higashida RT, Starkman S, Gobin YP, Multi MERCI investigators. Frei D, Grobelny T, Hellinger F, huddle D, Kidwell C, Koroshetz W, marks M, Nesbit G, Silverman IE. Mechanical thrombectomy for acute ischemic stroke: Final results of the multi MERCI trial. Stroke. 2008; 39(4):1205–1212. [PubMed: 18309168]

Smith WS, Lev MH, English JD, Camargo EC, Chou M, Johnston SC, Gonzalez G, Schaefer PW, Dillon WP, Koroshetz WJ, Furie KL. Significance of large vessel intracranial occlusion causing acute ischemic stroke and TIA. Stroke. 2009; 40(12):3834–3840. [PubMed: 19834014]

Wang W. Magnetic resonance-guided active catheter tracking. Magn Reson Imaging Clin N Am. 2015; 23(4):579–589. [PubMed: 26499276]

Wendt M, Wacker FK. Visualization, tracking, and navigation of instruments for magnetic resonance imaging-guided endovascular procedures. Top Magn Reson Imaging. 2000; 11(3):163–172. [PubMed: 11145208]

Mozaffarian D, Benjamin EJ, Go AS, Arnett DK, Blaha MJ, Cushman M, Das SR, de Ferranti S, Despres JP, Fullerton HJ, Howard VJ, Huffman MD, Isasi CR, Jimenez MC, Judd SE, Kissela BM, Lichtman JH, Lisabeth LD, Liu S, Mackey RH, Magid DJ, DK MG 3rd, Mohler ER, Moy CS, Muntner P, Mussolino ME, Nasir K, Neumar RW, Nichol G, Palaniappan L, Pandey DK, Reeves MJ, Rodriguez CJ, Rosamond W, Sorlie PD, Stein J, Towfighi A, Turan TN, Virani SS, Woo D, Yeh RW, Turner MB, American Heart Association Statistics Committee, Stroke Statistics Subcommittee. Heart disease and stroke statistics-2016 update: A report from the american heart association. Circulation. 2016 Jan 26; 133(4):e38–360. [PubMed: 26673558]

Zuehlsdorff S, Umathum R, Volz S, Hallscheidt P, Fink C, Semmler W, Bock M. MR coil design for simultaneous tip tracking and curvature delineation of a catheter. Magn Reson Med. 2004; 52(1): 214–218. [PubMed: 15236390]

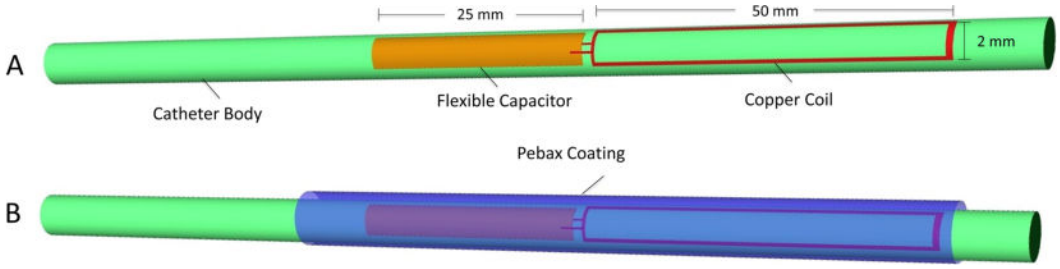

Fig. 1.

Resonant Catheter Design: The wireless resonant circuit, consisting of a single loop copper coil connected to a tunable flexible printed circuit board capacitor (55–100 pF), is tuned to the Larmor frequency of 63.89 Mhz and embedded in distal tip of a polyether ether ketone (PEEK) fiber thread catheter. The catheter is then coated with a protective Pebax layer

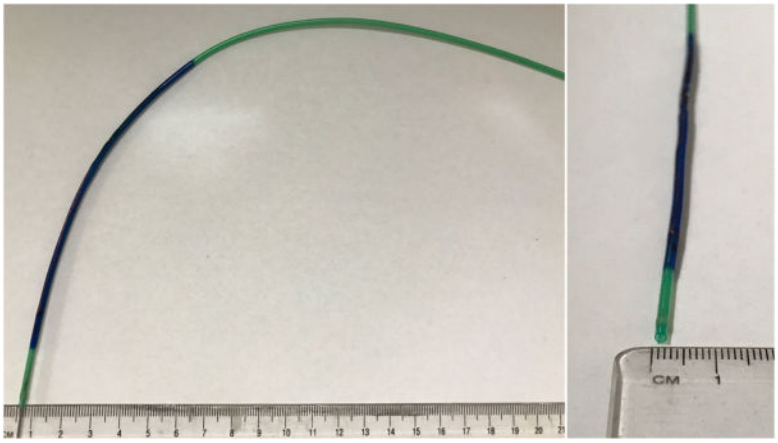

Fig. 2.

The PEEK fiber used to braid the catheter allowed for adequate deflection and flexibility for the resonant circuit catheter system to make vascular turns. The figure demonstrates the catheter system's mechanical properties and provides a cross-sectional view of the lumen

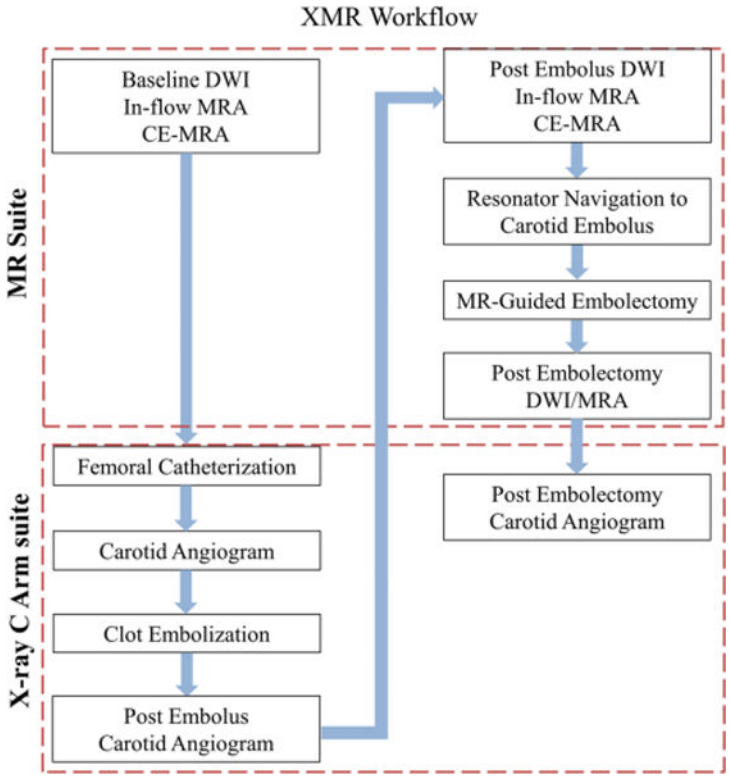

Fig. 3.

The experimental workflow in the clinical hybrid interventional XMR suite. All experiments were done with an Achieva 1.5 T clinical MR scanner and an Integris V5000 C-arm DSA system (Philips Healthcare, Best, The Netherlands)

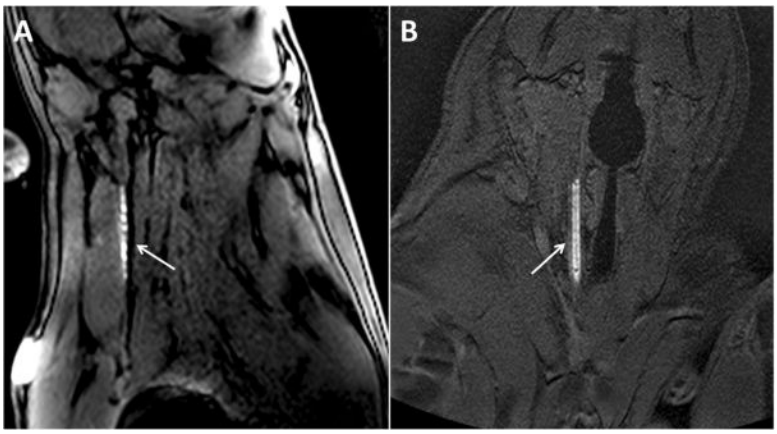

Fig. 4.

Demonstration of resonant catheter system visualization during active image tracking and across each orientation of navigational scan. The arrows point to the resonant marker catheter system. **a** Balanced steady-state free precession (bSSFP) sequence (TE = 2 ms, TR = 3.9 ms, Flip Angle = 10°, Slice thickness = 8 mm, FOV (cm) = 28 × 28, Slice orientation = sagittal) **b** Gradient echo (GRE) (TE = 1.7 ms, TR = 5.3 ms, Flip Angle = 10°, Slice thickness = 5 mm, FOV (cm) = 26 × 26, Slice orientation = coronal)

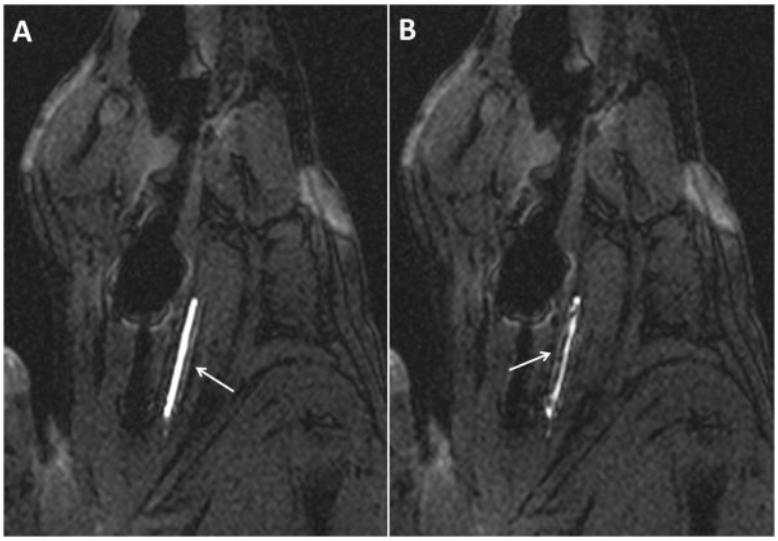

Fig. 5.

Active image tracking under bSSFP sequence during (**a**) navigation to occluded carotid artery and (**b**) clot aspiration into lumen of catheter, noted as filling defect. The arrows indicate resonant marker catheter system

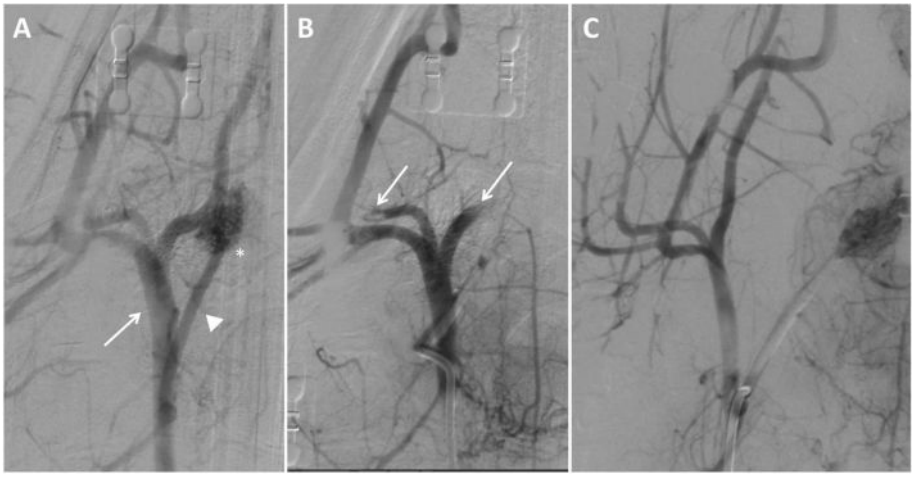

Fig. 6.

Digital subtraction angiography (DSA) imaging of right carotid vasculature from a single experiment. (**a**) Baseline start of study with the arrow pointing to the external carotid artery (ECA) and the asterisk identifying the ascending pharyngeal artery (APA) supplying the rete mirabile. (**b**) Post clot occlusion of carotid vasculature showing absent blood flow to the APA and rete mirabile with arrow identifying occlusion of blood flow to branches of the ECA. (**c**) Post embolectomy through manual aspiration identifying patent ECA, APA, and rete mirabile

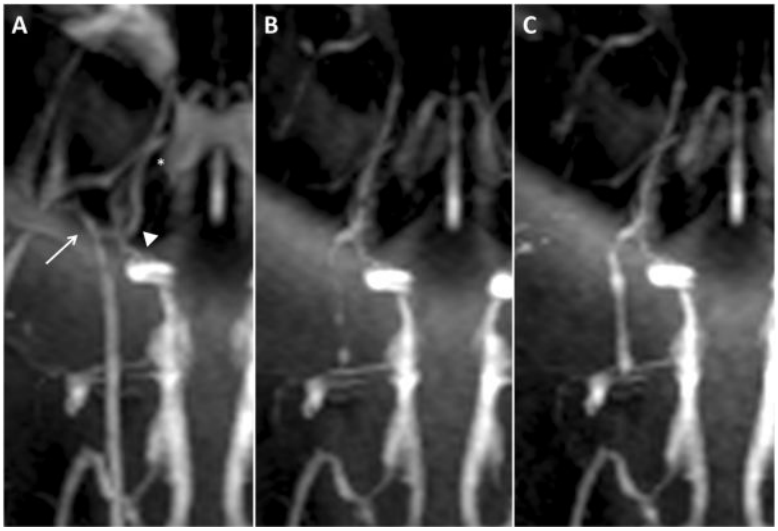

Fig. 7.

Magnetic resonance angiography imaging of the same selected right carotid vasculature as demonstrated in fig. 5. (**a**) Baseline start of study with arrow identifying the ECA, arrowhead identifying the APA, and asterisk identifying the rete mirabile. (**b**) Post clot occlusion MRA of carotid vasculature with absent ECA blood flow, and filling defects noted in the ICA and rete mirabile. (**c**) Post embolectomy through manual aspiration with return of blood flow to branches of the ECA and improving filling to the APA and rete mirabile

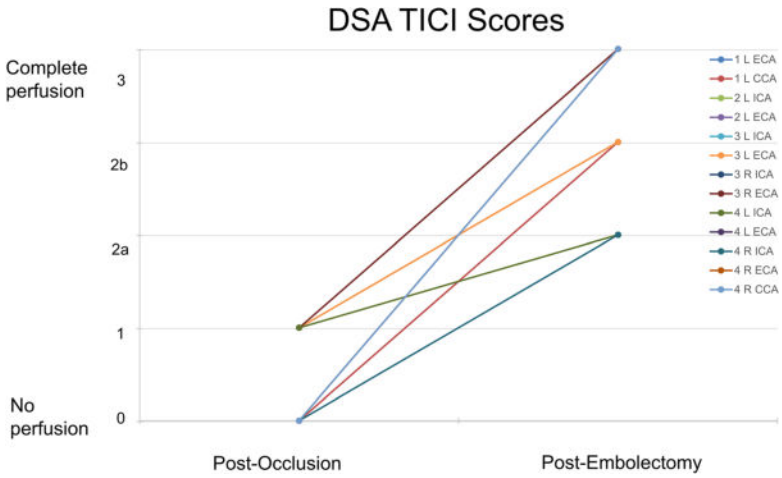

Fig. 8.

Thrombolysis in Cerebral Infarction scores as analyzed via DSA during clot occlusion and recanalization post embolectomy for each artery

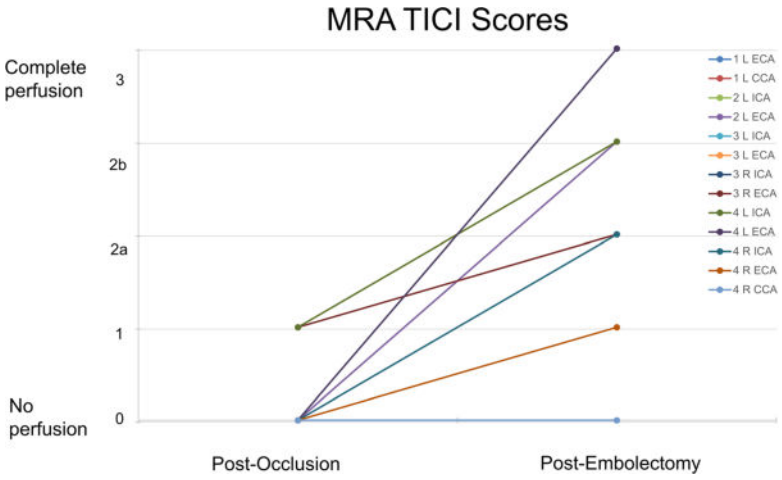

Fig. 9.

Thrombolysis in Cerebral Infarction scores as analyzed via CE-MRA during clot occlusion and recanalization post embolectomy for each artery. (TE = 1.5 ms, TR = 5.3 ms, Flip angle = 40°, Slice thickness = 3 mm)

Table 1

MR sequence names and parameters

MRI sequence parameters					
Sequence Name	**3D MRA**	**DWI**	**In-flow MRA**	**bSSFP**	**GRE**
Echo time, TE (ms)	1.5	65.2	6.9	2	1.7
Repetition Time, TR (ms)	5.3	3000	23	3.9	5.3
Flip Angle (°)	40	90	22	10–20	5–20
FOV (cm)	24 × 24	22 × 22	15 × 15	28 × 28	26 × 26
Frame Rate (fps)				1.5	
Slice Thickness (mm)	3	3	1.5	8	5
# of slices	80	31	120	1	5
Slice Orientation	Coronal	Axial	Axial	Sagittal/Coronal	Sagittal/Coronal